SEMARAK ILMU PUBLISHING

Journal of Advanced Research in Applied Mechanics

Journal homepage:
https://semarakilmu.com.my/journals/index.php/appl_mech/index
ISSN: 2289-7895

Bond Model for High Calcium Fly Ash Geopolymer Concrete

Hamdi Abdulrahman[1,*], Rahimah Muhamad[1], Ahmad Azim Shukri[2], Tariq Hassan Rasheed[3]

[1] Razak Faculty of Technology and Informatics, Universiti Teknologi Malaysia, Jalan Sultan Yahya Petra 54100 Kuala Lumpur, Malaysia
[2] Construction Research Centre, School of Civil Engineering, Faculty of Engineering, Universiti Teknologi Malaysia, 81310 Johor Bahru, Johor, Malaysia
[3] Department of Civil Engineering, Universiti Kebangsaan Malaysia (UKM), 43600 Bangi, Selangor, Malaysia

ARTICLE INFO

Article history:
Received 19 December 2023
Received in revised form 14 February 2024
Accepted 28 February 2024
Available online 30 April 2024

Keywords:
Bond strength; geopolymer; sustainability

ABSTRACT

Concrete industries and researchers have devoted great efforts to promoting sustainability in the construction sector. This includes finding innovative alternatives to OPC concrete to ensure environmental sustainability and prevent the depletion of natural resources. The present research explained the steps to develop a bond stress-slip model for high calcium fly ash (HCFA) geopolymer concrete based on the experimental results in the literature. This model is based on the concrete compressive strength (f_c), concrete cover (C_c), and bar diameter (d_b), which are considered the most influential parameters on the bond response between the reinforcement and surrounding concrete. The regressed model shows a quite accurate prediction of the bond behaviour of HCFA, particularly those with high strength. The slight difference was attributed to the difficulty in identifying the exact values of Slips (δ_{r1} and δ_{r2}).

1. Introduction

Concrete is a widely used construction material, with the most commonly used binder for concrete being Ordinary Portland Cement (OPC). The production of OPC utilizes a massive amount of national resources and increases the carbon footprint on our planet [1-4]. Therefore, significant efforts have been made to examine the possibility of using fly ash waste with low carbon footprints to replace OPC, such as alkali–activated binders [5-14]. Alkali–activated binders are produced by mixing fly ash (FA) with an alkaline solution (AA). The alkaline solution is a combination of sodium hydroxide (NaOH) and sodium silicate (Na_2SiO_3) [13]. Alkali–activated binders have several advantages over OPC, such as better compressive and splitting strength [7-9], strong resistance to chemical attacks [15], excellent fire resistance [16], and good repairing agent [13,17].

The most important component of alkali–activated binders is fly ash, which represents the product of burning coals in power plants. Fly ash can be categorized into two classes as described by ASTM C618 [18], which are high calcium fly ash (HCFA) and low calcium fly ash (LCFA). HCFA contains 50% of the pozzolanic compounds, while LCFA contains at least 70% pozzolanic compounds. Another

* *Corresponding author.*
E-mail address: Hamdialsofi@gmail.com

https://doi.org/10.37934/aram.116.1.2436

significant difference between both types is the calcium content, where HCFA is characterized by higher calcium oxide (>10% by mass) than LCFA [12]. Furthermore, HCFA is produced normally from the burning of lignite and sub–bituminous coals and usually has pozzolanic properties as well as cementitious properties [10], whereas LCFA is produced from burning bituminous and anthracite coals [19]. Therefore, the chemical compositions of the FAs differ according to the nature of the coal source it was produced. Because of the cementitious properties of FA and its low carbon footprint, it can be a promising binder for concrete, and hence, a clear understanding of the structural behaviour and bond performance is required.

The bond between concrete and steel bars governs the structural response of the reinforced concrete. This bond can be defined as the chemical adhesion, interlocking, and frictional resistance between the steel reinforcement and the surrounding concrete to convey the exerted stress [20]. Bond strength affects the embedded length of the steel bar and hence, the structural member's loading capacity and crack opening and spacing [21]. Meanwhile, Bond performance is greatly dominated by the compressive and tensile strength of concrete as well as the steel rebar properties [20]. Thereby, ACI-408R [20] highlighted the importance of understanding the bond behaviour of reinforced concrete before the analysis and design of the structural members. Also, there is a lack of understanding of the bond response of HCFA geopolymer concrete. Therefore, before introducing the alkali–activated concrete for actual engineering applications, understanding the real bond performance of this new concrete must be ascertained to avoid unsafe design. In response, the current study shows the steps to develop the bond strength model for HCFA geopolymer concrete based on the experimental results in the literature. Such a study is intended to examine the potential of HCFA geopolymer concrete as an alternative to OPC concrete, thus, encouraging innovation, preserving natural resources, and promoting environmental sustainability. This is because the conventional (OPC) OPC concrete has contributed significantly to greenhouse gas emissions and the depletion of natural resources. Furthermore, the current study is also a step forward in decreasing the overall cost of construction as geopolymer concrete is manufactured from industrial waste materials

2. Methodology

2.1 Steps for Developing the Bond Stress-Slip Model for HCFA Geopolymer Concrete

The current study used the experimental bond stress-slip results reported in the literature [22] and shown again in Table 1 to mathematically develop a bond stress-slip model for HCFA geopolymer concrete using Origin Pro 8.5 software. This model can be used for establishing a model for the bond between reinforcement and HCFA geopolymer concrete, and it is similar to those available models in the literature for OPC concrete [23]. The parameters used in the models were the concrete strength (f_c), concrete cover (Cc) and reinforcement bar diameter (d_b).

Table 1
Bond properties of HCFA geopolymer concrete [22]

Specimen ID.	f_c (MPa)	C_c/d_b ratio	τ_{max} (MPa)	δ_{r1} (mm)	δ_{r2} (mm)	τ_{fr} (MPa)
M5–FA 10	41.6	4.5	22.1	0.8	6.0	1.5
M5–FA 12	42.4	3.7	18.9	0.7	6.0	1.4
M5–FA 16	43.2	2.6	18.9	0.9	6.1	1.6
M8–FA 10	33.6	4.5	14.6	0.5	6.0	2.5
M8–FA 12	38.4	3.7	18.2	1.0	5.5	3.3
M8–FA 16	39.2	2.6	14.7	0.6	6.1	1.25
M9–FA 10	26.4	4.5	13.2	1.1	6.2	4.6
M9–FA 12	24	3.7	9.9	0.6	6.0	1.1
M9–FA 16	32	2.6	16.1	0.7	6.0	4.12

Notation: C_c/d_b= concrete cover to diameter ratio

3. Results and Discussion

3.1 Modes of Failure of Fly Ash Geopolymer Concrete

From visual observation, it can be reported that the failure modes of concrete cubes were quasi-brittle, which is characterized by a gradual decay of loads. A sample of the failure modes obtained in the current study is shown in Figure 1. It should be noted that the obtained failure mode is a satisfactory failure as all the cube faces cracked approximately equally, generally with little damage to faces in contact with the machine plate. This is a good indication of the uniform pressure from the machine on the specimens.

Fig. 1. Cube specimens failure mode

The failure modes of splitting tensile specimens are shown in Figure 2, where all specimens were split into halves in quasi-brittle behaviour, which is slow and soft due to the improved composition of the HCFA geopolymer concrete matrix [24]. This type of failure was visually observed among all the splitting tensile specimens, and this failure is a common failure mode in OPC concrete.

Fig. 2. The failure mode of splitting tensile specimens

Most of the pullout specimens failed by splitting concrete cover, as seen in Figure 3. It is worth noting that the embedment length of 5 times the reinforcement bar diameter used for all specimens in the present study could be a possible reason for the concrete splitting reported by CEB-FIP [23]. and Pop *et al.,* [21]. The used embedment length was sufficient to develop high radial stresses on the steel ribs resulting in wider longitudinal cracks that propagated to the external surface of the concrete [25]. A similar conclusion on the effects of embedment length on the pullout failure mode can also be seen in the experimental study undertaken by Topark–Ngami *et al.,* [26], where all pullout specimens of HCFA concrete underwent concrete splitting.

Fig. 3. The failure mode of splitting tensile specimens

3.2 Ultimate Bond Strength (τ_{max})

The bond strength of OPC concrete can be predicted directly using the empirical formulas available in the literature [27,28]. Several attempts were also carried out to develop formulas for fly ash geopolymer concrete [26,29,30] and presented in Eq. (1) to Eq. (5). These models were developed for OPC and fly ash geopolymer concrete [26-29,31] and were examined to predict the bond strength of HCFA reported by [22]. This can be shown graphically in Figure 4. This validation reveals that the models by Orangun *et al.,* [27] and Hadi [28] always tend to underestimate the maximum bond strength of HCFA geopolymer concrete because these expressions were developed based on OPC concrete which might exhibit a lesser bond strength. Meanwhile, the models by Dahou *et al.,* [29] and Kim and Park [31] gave a higher prediction value because these models were developed based on LCFA geopolymer concrete that underwent heat curing, which differs from the ambient curing

employed in the present study. It is clear that the model by Topark-Ngarm *et al.,* [26] gave a close prediction with only a 20% underestimation, and this agreement was attributed to the HCFA binder and ambient curing regime considered in their study. To avoid unsafe or suboptimal calculation of bond strength, the current study has regressed a model (Figure 9) to predict the maximum bond strength in term of compressive strength and C_c/d_b ratio as given in Eq. (6). By referring to this Equation, one can see that the correlation coefficient (R^2) between the vertical and horizontal variables has a value of 0.40. The slight scatter of the results in the graph was because of considering only one variable in the model development among many other variables such as the embedment length and reinforcement ribs. Although the lower value of R^2 resulted from regressing a small database, it is suggested that the developed equations could be served as a basis for developing more generic model in future.

$$\frac{\tau_{max}}{\sqrt{f_c}} = 0.083045\left(1.22 + 3.23\,\frac{C_c}{d_b} + 53.0\,\frac{d_b}{l_d}\right) \tag{1}$$

$$\frac{\tau_{max}}{\sqrt{f_c}} = 2.07 + 0.2\,\frac{C_c}{d_b} + 4.15\,\frac{d_b}{l_d} \tag{2}$$

$$\frac{\tau_{max}}{\sqrt{f_c}} = 0.083045(22.8 - 0.208\,\frac{C_c}{d_b} - 38.212\,\frac{d_b}{l_d}) \tag{3}$$

$$\tau_{max} = 2.12\sqrt{f_c} \tag{4}$$

$$\tau_{max} = 3.83\sqrt{f_c} \tag{5}$$

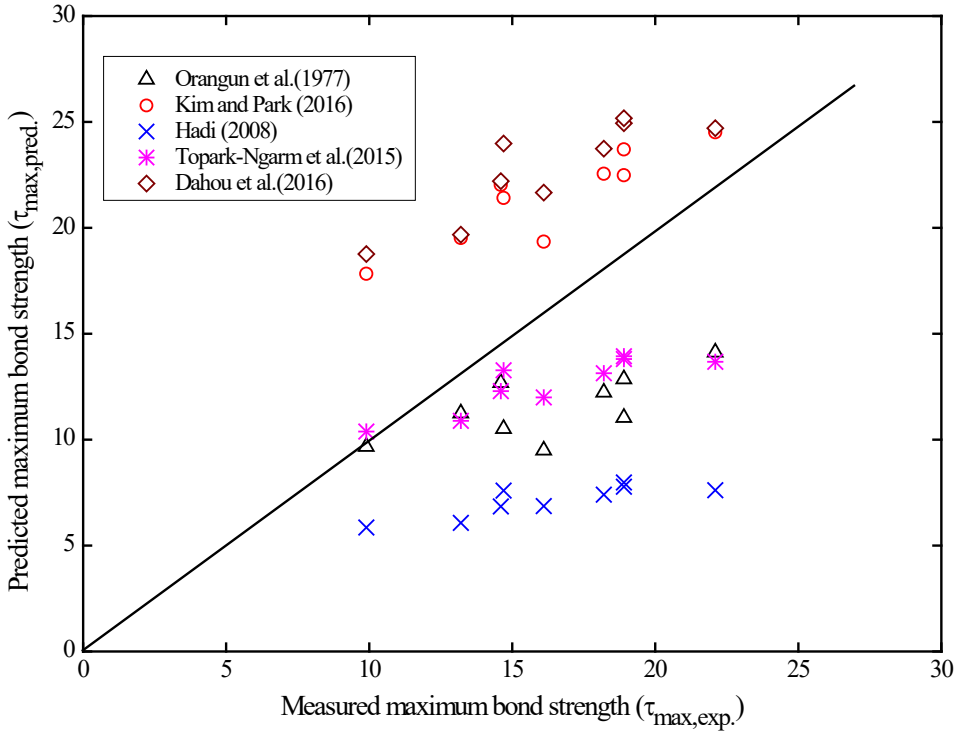

Fig. 4. Comparison between the experimental and predicted maximum bond

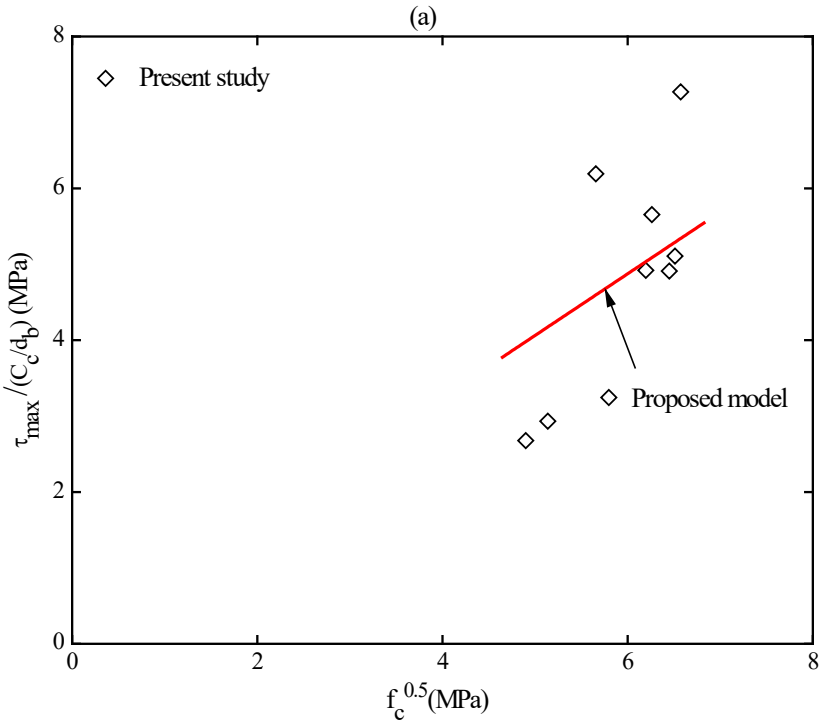

Fig. 5. The influence of compressive strength and confinement on ultimate bond strength obtained in the current study

$$\tau_{max} = 0.81\sqrt{f_c}\left(\frac{C_c}{d_b}\right), R^2 = 0.40 \quad (6)$$

3.3 Slip at Maximum Stress (δ_{r1})

The slips (δr1) corresponding to the ultimate bond strength are presented in Table 1. It can be noticed that the slips (δ_{r1}) range from 0.45 mm to 1.12 mm, with an average of 0.75 mm. These results agree with that observed by Ganeshan *et al.,* [32], confirming that the slip values of the blended HCFA geopolymer concrete were lower than OPC counterparts. This was attributed to the superior bond properties of HCFA concrete, which prevented the steel bar from slipping when the tension load was applied to the steel bar. It is worth mentioning that the slip value recommended by CEB–FIB [23] for OPC concrete is 1mm, indicating a strong bond performance of HCFA geopolymer concrete. The results of the slip (δ_{r1}) reported in Table 1 were regressed to develop a model as in Figure 6, and the slip (δ_{r1}) was described in Eq. (7). By referring to Figure 6 and the R2 values (0.1), the scatter of the results demonstrated that τmax does not significantly influence δr1, and it only has a marginal effect on the slip (δr1). This is because the slip (δr1) is controlled substantially by reinforcement ribs [33]. However, the relationship between δ_{r1} and reinforcement ribs was not developed due to the absence of information about the reinforcement ribs that differ from one reinforcement manufacturer to another. Thus, similar to the approach in literature [23,33,34], in deriving the bond model for HCFA geopolymer concrete, the proposed δ_{r1} value was taken as a constant value of 0.75 mm. This value equals the average of δ_{r1} obtained experimentally and shown in Table 1.

$$\delta_{r1} = 0.015\tau_{max} + 0.53, R^2 = 0.1 \quad (7)$$

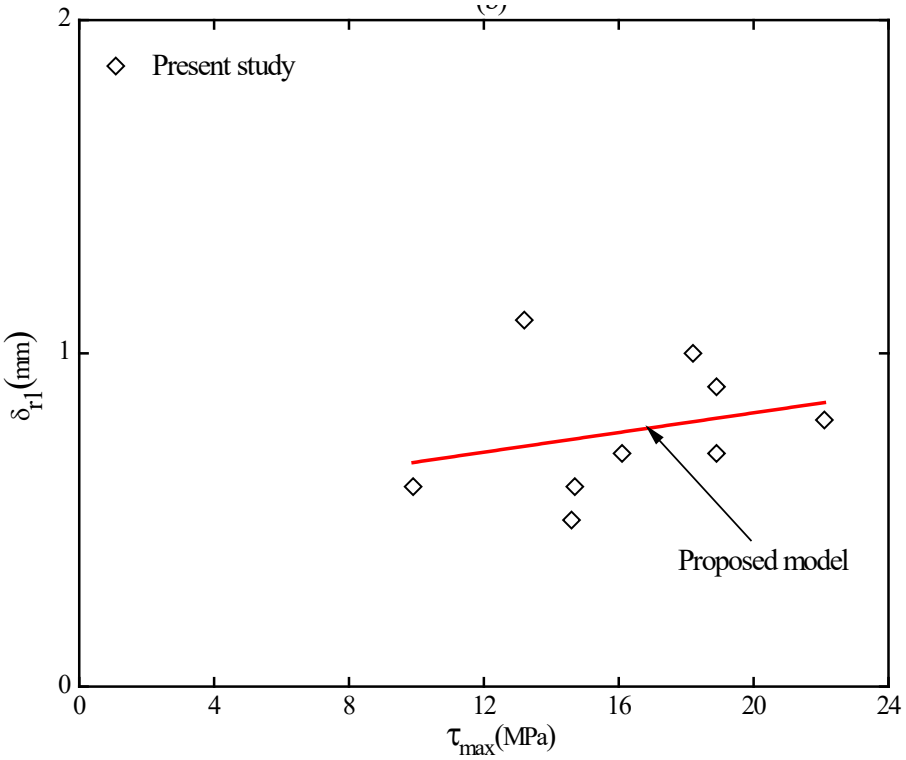

Fig. 6. The effect of ultimate bond strength (τ_{max}) on the slip (δ_{r1})

3.4 Frictional Bond Strength and Maximum Slip

Frictional bond strength (τ_{fr}) is the residual component in the bond stress-slip curve. It is dependent on the friction between the steel bar surface and the neighbouring concrete. The frictional bond strength of HCFA geopolymer concrete is summarized in Table 1. Its relationship with the highest bond strength is graphically presented in Figure 7 and expressed mathematically by Eq. (8). It is evident from the figure that τ_{max} has a marginal effect on τ_{fr}, where its increase does not significantly increase τfr value. It is worth mentioning that M9-FA-10 was not considered in the analysis during the regression. Hence, it is expected that the results from this specimen were affected by an error during the lab work and hence, were not used in the regression. The mathematical expression is given by Eq. (8), where R^2 value is 0.1. This small value does not necessarily indicate the dispersion of the results, but it was due to the small database used in the regression.

$$\tau_{fr} = 0.1\tau_{max} + 0.64, R^2 = 0.1 \quad (8)$$

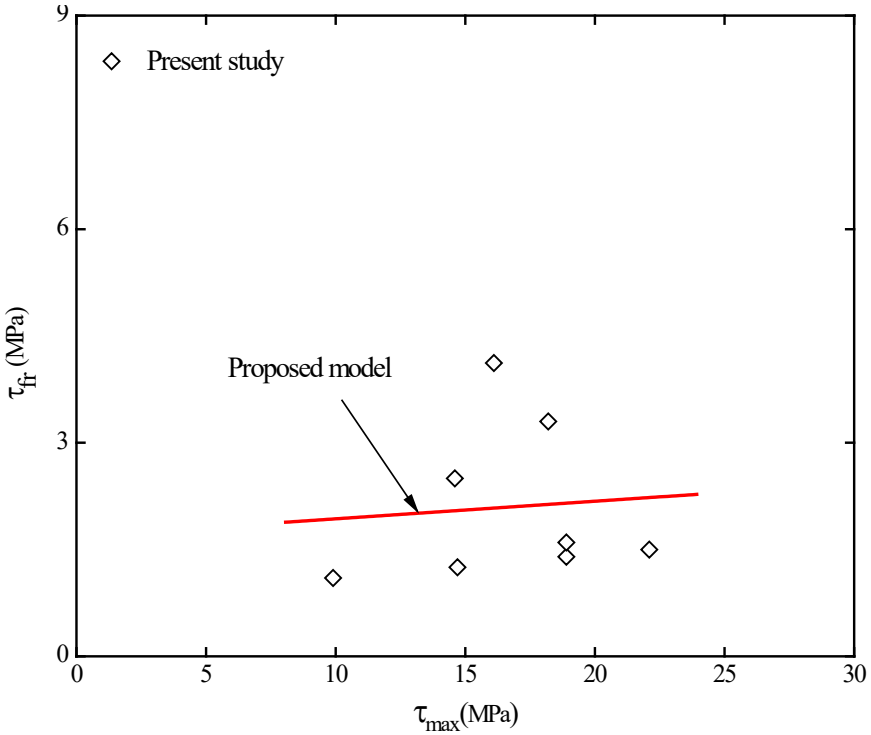

Fig. 7. The relationship between frictional and ultimate bond strength

The maximum slip (δ_{r2}) is where the frictional bond stress commences. It is summarized in Table 1 and plotted graphically as a function of the ultimate bond strength in Figure 8, where the slip shows a minimal dependency on the maximum bond strength. Although a relationship between τmax and δ_{r2} is proposed here, the scatter of results in Figure 8 with R^2 values (0.02) suggests that τmax has a marginal effect on δ_{r2}. This is primarily because reinforcement slip, in general, is governed by the reinforcement bar geometry (ribs) [33]. However, no relationship was developed between δ_{r2} and the reinforcement bar geometry (ribs) due to the unavailability of the rib geometry as well as the involved elongation during the loading. Thus, the δ_{r2} was proposed by averaging the experimental slip given in Table 1 to be used for developing the bond stress-slip model for HCFA geopolymer concrete, which is similar to the approach followed in the literature [23,33,34].

$$\delta_{r3} = 0.01\tau_{max} + 2.025, R^2 = 0.02 \quad (9)$$

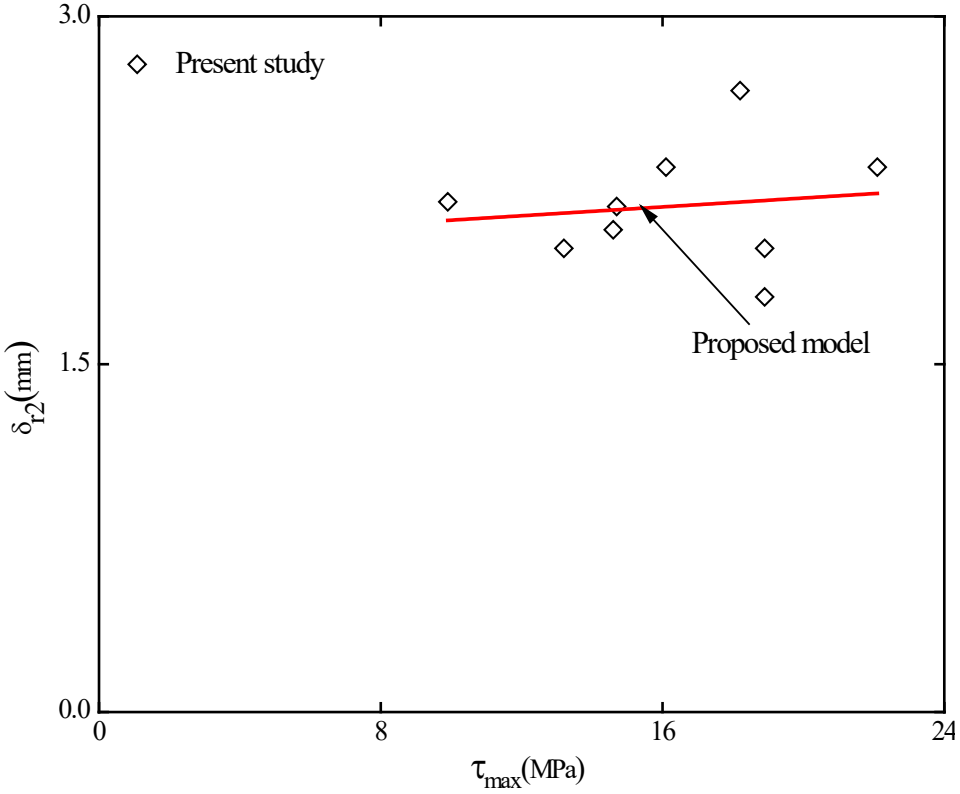

Fig. 8. The effects of ultimate bond strength on maximum slip

3.5 Bond Stress Slip Mechanism

As shown in Figure 10, The bond stress slip curve can be generally divided into five phases; linear, nonlinear, splitting stage, nonlinearly deterioration of bond capacity, and the constant frictional bond component. This is generally similar to the stages described in the literature [35]. The first stage usually is resulted from the chemical components between the steel bar and the sounding concrete, which diminishes when the bar starts to slip. On the other hand, the formation of the nonlinear stage is due to the intensive internal cracks formed around the steel bar, and this phase fails when the maximum bond is achieved. This high bond resistance is generated due to the interlocking between the concrete and the reinforcement. The remaining phases following the concrete splitting are minimal and produce lesser bond resistance due to the frictional force between the top surface of the reinforcing bar and the surrounding concrete.

3.6 Bond Model Based on the Experimental Results

Based on CEB–FIB [23] and the equations shown in previous sections on the bond response of HCFA, a model for the bond response of HCFA geopolymer concrete was proposed, as illustrated in Figure 9. The ascending, ultimate, softening, and residual parts of the bond-slip were described by Eq. (10) to Eq. (14). The bond stress-slip developments were based on the regression performed in the earlier described sections. For instance, the horizontal axis represents the slip of the reinforcement that includes δr1 and δr2. In a similar way to CEB–FIB [23] and the conclusions drawn earlier for both δr1 and δr2 were proposed as 0.75mm and 2mm, respectively. This is primarily because the slip of reinforcement is governed by ribs and is not affected by maximum bond strength. The vertical bond stress corresponding to these slips is known as maximum bond stress (τmax), and frictional bond stress (τfr) and their regressed equations were established earlier. In addition, the

ascending branch (slip < δr1) was developed by amending the equation of CEB–FIB [23] until it gave the best fit for the experimental results. Thus, for the ascending branch of the model (slip < δr1), Eq. (10) should be used. Similarly, the descending branch of the model (δr1< slip < δr2) is also calculated based on Eq. (11) which is similar to that of OPC concrete provided by CEB–FIB [23] due to its ability to predict the descending branch of the experimental results.

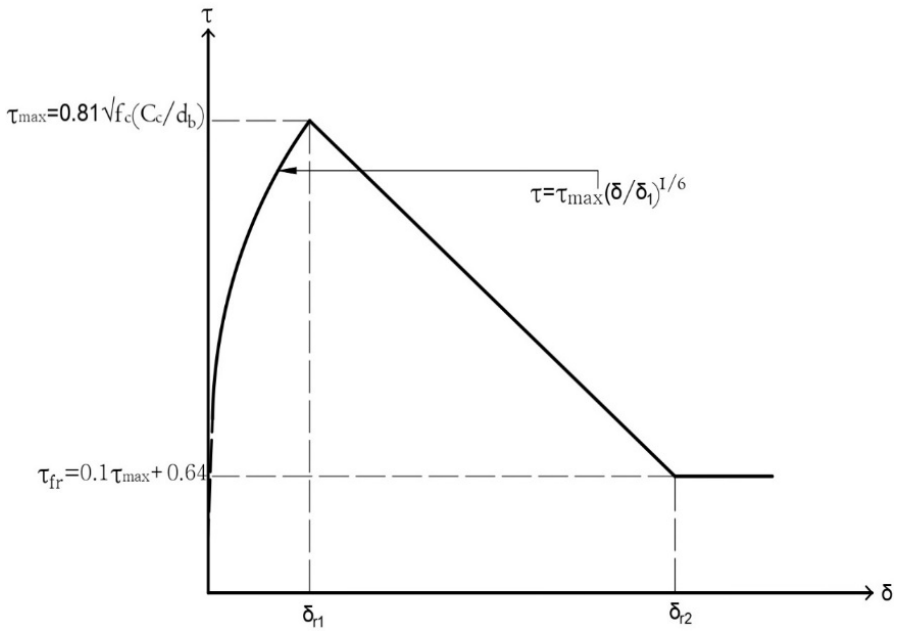

Fig. 9. Bond stress-slip model based on the experimental results only

$$\tau = \tau_{\max} \left(\frac{\delta_r}{\delta_{r1}}\right)^{\frac{1}{6}} \quad For \;\; \delta_r \leq \delta_{r1} \tag{10}$$

$$\tau = \tau_{\max} - (\tau_{\max} - \tau_{fr}) \left(\frac{\delta_r - \delta_{r1}}{\delta_{r2} - \delta_{r1}}\right) \text{ for } \delta_r > \delta_{r1} \text{ and } \delta_r \leq \delta_{r2} \tag{11}$$

$$\tau = \tau_{fr} \text{ for } \delta_r > \delta_{r2} \tag{12}$$

where

$$\tau_{\max} = 0.81 \sqrt{f_c} \left(\frac{C_c}{d_b}\right) \tag{13}$$

$$\tau_{fr} = 0.1\tau_{\max} + 0.64 \tag{14}$$

and the proposed δ_{r1} and δ_{r2} values were 0.75 mm and 2 mm, respectively.

The bond-slip response predicted by the proposed model was compared graphically with the experimental bond response in Figure 10. The proposed bond response agrees well with the experimental bond response, and the slight difference was attributed to the difficulty in identifying the exact values of δ_{r1} and δ_{r2}. Furthermore, one reason for the accurate prediction of the model was because the model is calibrated and validated using the same database, and this limitation was avoided by developing a more generic model in the following section. Finally, the model accurately predicted the maximum bond strength for pullout specimens with high compressive strength, particularly manufactured from M5 and M8. Meanwhile, it showed less accuracy in predicting the

bond strength of pullout specimens manufactured from M9, which has a lower compressive strength. This indicates that reducing the compressive strength below a specific limit could result in marginal effects on bond strength.

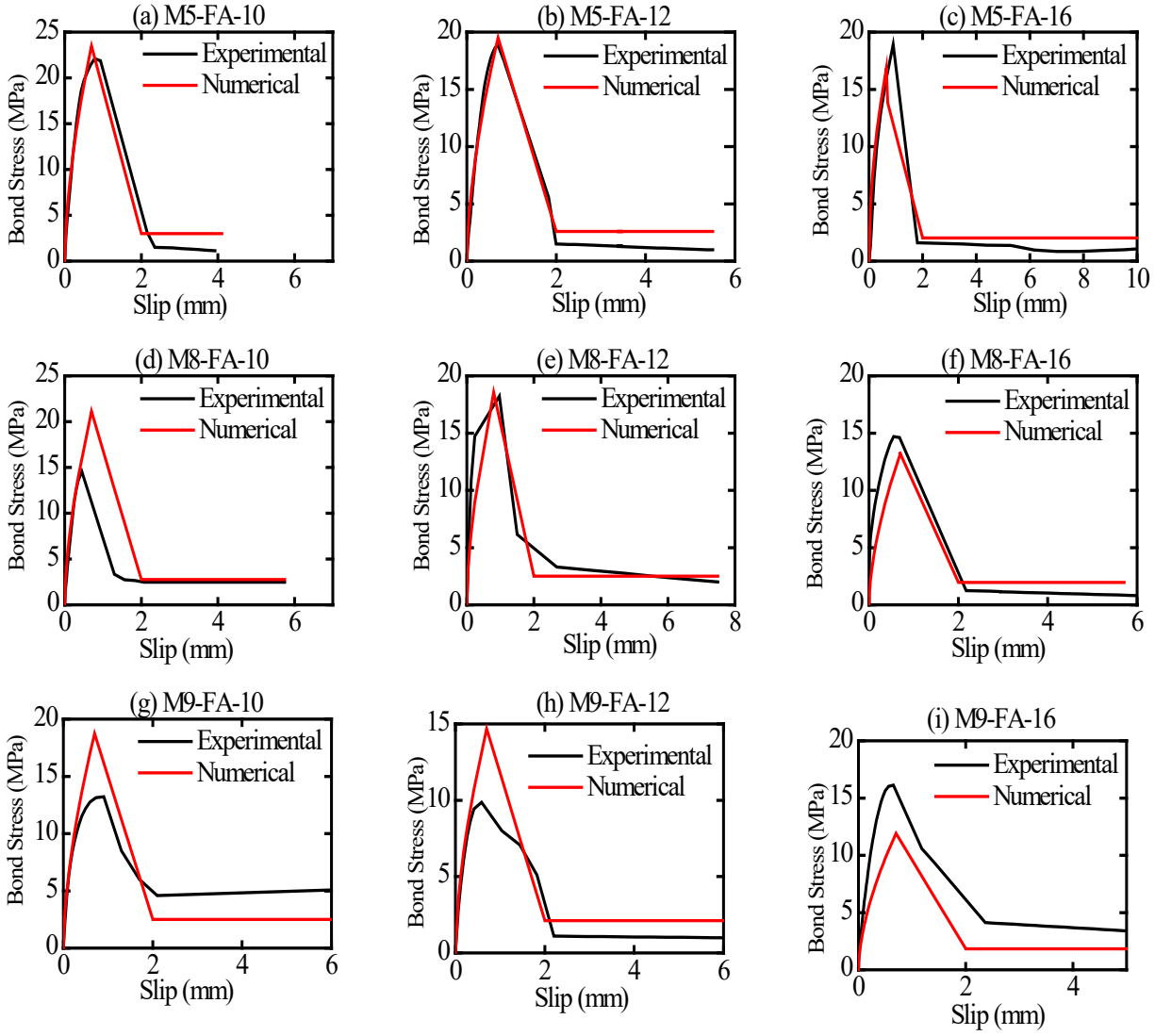

Fig. 10. Graphical comparisons of the experimental results with the predicted bond stress-slip

4. Conclusion

Increasing awareness among people has shifted the research direction towards finding a sustainable construction material that prevents the environment for future generations and reduces the carbon footprints of OPC concrete. Thus, the current study aims to show the steps in developing the bond-slip model for high calcium fly ash geopolymer concrete that is necessary for estimating the interaction between reinforcement and surrounding concrete. The initial step was to examine the possibility of using the existing mathematical models in the literature to estimate the maximum bond capacity. Then, the bond stress-slip results were collected from the literature and regressed to develop the bond models, which could predict the bond response of HCFA geopolymer concrete. This model could serve as a benchmark to develop a more detailed model for flexural members.

Acknowledgement

The authors gratefully acknowledge the Universiti Teknologi Malaysia [Grant No: Q.K130000.2556.21H60] for funding this project.

References

[1] Turner, Louise K., and Frank G. Collins. "Carbon dioxide equivalent (CO2-e) emissions: A comparison between geopolymer and OPC cement concrete." *Construction and building materials* 43 (2013): 125-130. https://doi.org/10.1016/j.conbuildmat.2013.01.023

[2] Ha, Chin Yee, Terh Jing Khoo, and Jia Xuan Loh. "Barriers to green building implementation in Malaysia: A systematic review." *Progress in Energy and Environment* (2023): 11-21. https://doi.org/10.37934/progee.24.1.1121

[3] Yong, Jiunn Boon, Lian See Tan, and Jully Tan. "Comparative life cycle assessment of biomass-based and coal-based activated carbon production." *Progress in Energy and Environment* (2022): 1-15. https://doi.org/10.37934/progee.20.1.115

[4] Yee, Ha Chin, Radzi Ismail, and Khoo Terh Jing. "The barriers of implementing green building in Penang construction industry." *Progress in Energy and Environment* (2020): 1-10.

[5] Abdulrahman, H., and R. Muhamad. "Effects of mix design parameters on compressive strength of high calcium fly ash geopolymer concrete." In *AIP Conference Proceedings*, vol. 2401, no. 1. AIP Publishing, 2021.

[6] Sani, M. F. A., R. Muhamad, and H. Abdulrahman. "Bond stress-slip of fly ash-based geopolymer concrete: A review." In *AIP Conference Proceedings*, vol. 2284, no. 1. AIP Publishing, 2020. https://doi.org/10.1063/5.0027235

[7] Sofi, M, J. S. J. Van Deventer, P. A. Mendis, and G. C. Lukey. "Bond performance of reinforcing bars in inorganic polymer concrete (IPC)." *Journal of Materials Science* 42 (2007): 3107-3116. https://doi.org/10.1007/s10853-006-0534-5

[8] Sarker, Prabir Kumar. "Bond strength of reinforcing steel embedded in fly ash-based geopolymer concrete." *Materials and structures* 44 (2011): 1021-1030. https://doi.org/10.1617/s11527-010-9683-8

[9] Chindaprasirt, Prinya, T. Chareerat, and Vute Sirivivatnanon. "Workability and strength of coarse high calcium fly ash geopolymer." *Cement and concrete composites* 29, no. 3 (2007): 224-229. https://doi.org/10.1016/j.cemconcomp.2006.11.002

[10] Guo, Xiaolu, Huisheng Shi, and Warren A. Dick. "Compressive strength and microstructural characteristics of class C fly ash geopolymer." *Cement and concrete composites* 32, no. 2 (2010): 142-147. https://doi.org/10.1016/j.cemconcomp.2009.11.003

[11] Li, Shucai, Fei Sha, Rentai Liu, Wei Li, Zhaofeng Li, and Guancong Wang. "Properties of cement-based grouts with high amounts of ground granulated blast-furnace slag and fly ash." *Journal of Materials in Civil Engineering* 29, no. 11 (2017): 04017219. https://doi.org/10.1061/(ASCE)MT.1943-5533.0002083

[12] Gomaa, Eslam, Simon Sargon, Cedric Kashosi, and Mohamed ElGawady. "Fresh properties and compressive strength of high calcium alkali activated fly ash mortar." *Journal of King Saud University-Engineering Sciences* 29, no. 4 (2017): 356-364. https://doi.org/10.1016/j.jksues.2017.06.001

[13] Gomaa, Eslam, Ahmed A. Gheni, Cedric Kashosi, and Mohamed A. ElGawady. "Bond strength of eco-friendly class C fly ash-based thermally cured alkali-activated concrete to portland cement concrete." *Journal of Cleaner Production* 235 (2019): 404-416. https://doi.org/10.1016/j.jclepro.2019.06.268

[14] Gomaa, Eslam, Ahmed Gheni, and Mohamed A. ElGawady. "Repair of ordinary Portland cement concrete using ambient-cured alkali-activated concrete: Interfacial behavior." *Cement and Concrete Research* 129 (2020): 105968. https://doi.org/10.1016/j.cemconres.2019.105968

[15] Liu, Kaiwei, Daosheng Sun, Aiguo Wang, Gaozhan Zhang, and Jinhui Tang. "Long-term performance of blended cement paste containing fly ash against sodium sulfate attack." *Journal of Materials in Civil Engineering* 30, no. 12 (2018): 04018309. https://doi.org/10.1061/(ASCE)MT.1943-5533.0002516

[16] Wongsa, Ampol, Athika Wongkvanklom, Duangkanok Tanangteerapong, and Prinya Chindaprasirt. "Comparative study of fire-resistant behaviors of high-calcium fly ash geopolymer mortar containing zeolite and mullite." *Journal of Sustainable Cement-Based Materials* 9, no. 5 (2020): 307-321. https://doi.org/10.1080/21650373.2020.1748741

[17] Gomaa, Eslam, Simon Sargon, Cedric Kashosi, Ahmed Gheni, and Mohamed A. ElGawady. "Mechanical properties of high early strength class c fly Ash-Based alkali activated concrete." *Transportation Research Record* 2674, no. 5 (2020): 430-443. https://doi.org/10.1177/0361198120915892

[18] ASTM Committee C-09 on Concrete and Concrete Aggregates. *Standard specification for coal fly ash and raw or calcined natural pozzolan for use in concrete*. ASTM international, 2013.

[19] Jiang, Xi, Yiyuan Zhang, Rui Xiao, Pawel Polaczyk, Miaomiao Zhang, Wei Hu, Yun Bai, and Baoshan Huang. "A comparative study on geopolymers synthesized by different classes of fly ash after exposure to elevated temperatures." *Journal of Cleaner Production* 270 (2020): 122500. https://doi.org/10.1016/j.jclepro.2020.122500

[20] Allen, John H., Anthony L. Felder, John F. McDermott, Atorod Azizinamini, Robert J. Frosch, Denis Mitchell, Gyorgy L. Balazs *et al.,* "Bond and Development of Straight Reinforcing Bars in Tension." (2003).
[21] Pop, Ioan, Geert De Schutter, Pieter Desnerck, and Traian Onet. "Bond between powder type self-compacting concrete and steel reinforcement." *Construction and Building Materials* 41 (2013): 824-833. https://doi.org/10.1016/j.conbuildmat.2012.12.029
[22] Abdulrahman, Hamdi, Rahimah Muhamad, Phillip Visintin, and Ahmad Azim Shukri. "Mechanical properties and bond stress-slip behaviour of fly ash geopolymer concrete." *Construction and Building Materials* 327 (2022): 126909. https://doi.org/10.1016/j.conbuildmat.2022.126909
[23] CEB-FIP, CEB-FIP, 2010.
[24] Golewski, Grzegorz Ludwik. "Evaluation of fracture processes under shear with the use of DIC technique in fly ash concrete and accurate measurement of crack path lengths with the use of a new crack tip tracking method." *Measurement* 181 (2021): 109632. https://doi.org/10.1016/j.measurement.2021.109632
[25] Maranan, Ginghis, Allan Manalo, Karu Karunasena, and Brahim Benmokrane. "Bond stress-slip behavior: case of GFRP bars in geopolymer concrete." *Journal of Materials in Civil Engineering* 27, no. 1 (2015): 04014116. https://doi.org/10.1061/(ASCE)MT.1943-5533.0001046
[26] Topark-Ngarm, Pattanapong, Prinya Chindaprasirt, and Vanchai Sata. "Setting time, strength, and bond of high-calcium fly ash geopolymer concrete." *Journal of materials in civil engineering* 27, no. 7 (2015): 04014198. https://doi.org/10.1061/(ASCE)MT.1943-5533.0001157
[27] Orangun, C. O., J. O. Jirsa, and J. E. Breen. "A reevaulation of test data on development length and splices." In *Journal Proceedings*, vol. 74, no. 3, pp. 114-122. 1977. https://doi.org/10.14359/10993
[28] Hadi, Muhammad NS. "Bond of high strength concrete with high strength reinforcing steel." (2008): 143.
[29] Dahou, Zohra, Arnaud Castel, and Amin Noushini. "Prediction of the steel-concrete bond strength from the compressive strength of Portland cement and geopolymer concretes." *Construction and Building Materials* 119 (2016): 329-342. https://doi.org/10.1016/j.conbuildmat.2016.05.002
[30] Kim, Jee Sang, and JongHo Park. "An experimental evaluation of development length of reinforcements embedded in geopolymer concrete." *Applied Mechanics and Materials* 578 (2014): 441-444. https://doi.org/10.4028/www.scientific.net/AMM.578-579.441
[31] Kim, Jee-Sang, and Jong Ho Park. "An experimental investigation of bond properties of reinforcements embedded in geopolymer concrete." *International Journal of Structural and Construction Engineering* 9, no. 2 (2015): 96-99.
[32] Ganeshan, Mahima, V. Sreevidya, L. Nirubanchakravarthy, and G. Sindhu. "Pull out behaviour of deformed steel bars in fly ash blended self compacting geopolymer concrete." *Revista Romana de Materiale* 48, no. 3 (2018): 346-354.
[33] Mo, Kim Hung, Phillip Visintin, U. Johnson Alengaram, and Mohd Zamin Jumaat. "Bond stress-slip relationship of oil palm shell lightweight concrete." *Engineering Structures* 127 (2016): 319-330. https://doi.org/10.1016/j.engstruct.2016.08.064
[34] Harajli, M., B. Hamad, and K. Karam. "Bond-slip response of reinforcing bars embedded in plain and fiber concrete." *Journal of materials in civil engineering* 14, no. 6 (2002): 503-511. https://doi.org/10.1061/(ASCE)0899-1561(2002)14:6(503)
[35] Cai, Jingming, Jinlong Pan, Jiawei Tan, and Xiaopeng Li. "Bond behaviours of deformed steel rebars in engineered cementitious composites (ECC) and concrete." *Construction and Building Materials* 252 (2020): 119082. https://doi.org/10.1016/j.conbuildmat.2020.119082